

Selected Paper

Two-Dimensional ^{1}H Spin-Exchange NMR Study of Molecular Arrangements in Diphenylhexatrienes

Shigenobu Hayashi* **and Yoriko Sonoda**[1]

Research Institute of Instrumentation Frontier, National Institute of Advanced Industrial Science and Technology (AIST), Tsukuba Central 5, 1-1-1 Higashi, Tsukuba, Ibaraki 305-8565

[1]Nanotechnology Research Institute, AIST, Tsukuba Central 5, 1-1-1 Higashi, Tsukuba, Ibaraki 305-8565

Received September 22, 2003; E-mail: hayashi.s@aist.go.jp

Molecular arrangements in crystalline solids of *p*,*p*′-disubstituted (1*E*,3*E*,5*E*)-1,6-diphenyl-1,3,5-hexatrienes (DPHs) have been studied by two-dimensional ^{1}H spin-exchange NMR. The mixing time dependence of the cross peak intensity has been analyzed, and the time constants representing proton spin exchange rates have been estimated. Data for methoxy derivative **1** demonstrate the presence of intermolecular spin exchange between triene protons and methoxy protons; thus one may conclude that a methoxy group is located close to a hexatriene chain of an adjacent molecule. On the other hand, there is no evidence of intermolecular spin exchange for formyl derivative **2**.

(1*E*,3*E*,5*E*)-1,6-Diphenyl-1,3,5-hexatriene (DPH) and its derivatives show a unique fluorescence behavior in solution. In our previous work,[1] absorption and fluorescence properties in the solid state have been studied for DPH and *p*,*p*′-disubstituted DPH derivatives (DPHs). The fluorescence properties are strongly dependent on the substituents. This can be attributed to strong charge-transfer type intermolecular interactions induced by the substituents. The compound **1** in Scheme 1 shows a structured and red-shifted fluorescence spectrum, while **2** shows a structureless and red-shifted spectrum.[1] Since DPHs have rodlike molecular structures, as shown in Scheme 1, the emission properties are strongly affected by intermolecular interactions and molecular arrangements. Since the X-ray diffraction study gave us very limited information on these compounds, we attempted to study the molecular arrangements by two-dimensional (2D) ^{1}H spin-exchange NMR. We reported only preliminary results without showing any spectra, and the results were described only qualitatively because no analysis was carried out at that time.[1] To our knowledge, this was the first study that investigated molecular arrangements in organic solids with unknown structures by means of 2D ^{1}H spin-exchange NMR.

Spin exchange (or spin diffusion) is one of the important phenomena in solid-state NMR spectroscopy because it gives us information including internuclear distances. 2D ^{1}H spin-exchange (or spin-diffusion) NMR and its related techniques have been applied to investigate homogeneity in polymer blends,[2–6] organic–inorganic hybrid materials,[7] membrane protein topology,[8] and inorganic silicates.[9] By use of proton spin exchange, these techniques can discriminate the following two cases; homogeneous mixing at molecular levels and formation of domains of each component. They can estimate a domain size of 1 to 500 nm.[4,10] It is sometimes difficult to determine the crystal structures of organic solids when good single crystals are not available. In those cases, the above NMR techniques are expected to be very useful to investigate molecular arrangements.

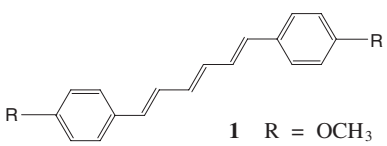

1 R = OCH_3
2 R = CHO

Scheme 1. Diphenylhexatrienes.

In the present work, we present the 2D ^{1}H spin-exchange NMR spectra of two DPHs shown in Scheme 1 and analyze them quantitatively. We estimate time constants representing spin exchange rates, which should correlate with internuclear distances. We can conclude that the two DPHs show much different molecular arrangements from each other. Thus, the 2D ^{1}H spin-exchange NMR can successfully be applied to study molecular arrangements in organic solids.

Experimental

Materials. Two DPHs were used in this work. The *p*,*p*′-disubstituted groups were methoxy (OCH_3) and formyl (CHO) groups for **1** and **2**, respectively, as shown in Scheme 1. They were in a powder form consisting of microcrystals and were the same as those used in the previous work.[1] The preparation method was described previously.[1]

NMR Measurements. ^{1}H NMR spectra were obtained with a Bruker ASX200 spectrometer, operating at a ^{1}H resonance frequency of 200.13 MHz. One-dimensional (1D) ^{1}H NMR spectra were obtained using the CRAMPS (Combined Rotation And Multiple-Pulse Spectroscopy) technique, where the BR-24 multipulse sequence was used in a quadrature detection mode.[11] The spinning rate was set at 1.6 kHz, the $\pi/2$ pulse width was 1.4 μs, the shorter pulse spacing was 2.6 μs, the repetition time was 8 s, the total number of the acquired data points was 1024, and the accumulation number was 16. One cycle time of BR-24 was 144 μs.

2D ^{1}H spin-exchange NMR spectra were measured with a pulse sequence similar to that in the literature,[2] where the quadrature

Published on the web December 10, 2004; DOI 10.1246/bcsj.77.2159

mode of BR-24 was used instead of MREV-8. 128 points were acquired in the f1 dimension, using States-TPPI.[12,13] The evolution period was incremented by 144 μs for each step. Other conditions were the same as those in the 1D CRAMPS measurements.

The ^{1}H chemical shifts were expressed with respect to pure tetramethylsilane (TMS), the higher frequency side being positive. They were calibrated by the signal position of silicone rubber (0.12 ppm from TMS)[14] mixed with the sample.

Results and Discussion

^{1}H CRAMPS Spectra. Figure 1 shows ^{1}H CRAMPS spectra of **1** and **2**. The BR-24 pulse sequence was used in this work because the resolution obtained by MREV-8 was not so good as to resolve the signal of aromatic protons from that of triene protons.

The spectrum of **1** shows peaks at 5.8, 4.4, and 3.1 ppm from TMS, whose integrated intensity ratios are about 6:1:3. In addition, the peak at 5.8 ppm has a shoulder at 5.1 ppm. The peaks are assigned based on solution NMR results and the integrated intensities.[1] The peak at 5.8 ppm is ascribed to aromatic protons, those at 5.1 and 4.4 ppm to triene protons, and that at 3.1 ppm to methoxy protons.

The spectrum of **2** has peaks at 9.3, 6.7, and 5.8 ppm. The peak at 9.3 ppm is assigned to formyl protons, that at 6.7 ppm to aromatic protons, and that at 5.8 ppm to triene protons and one type of aromatic protons.

All the peaks shift towards the lower frequency in solids when compared with those in solution. Among them, one signal of the triene protons in **1** has a very large low-frequency shift to 4.4 ppm, which might be caused by neighboring molecules having aromatic rings.

2D ^{1}H Spin-Exchange NMR Spectra. Figures 2 and 3 show 2D ^{1}H spin-exchange NMR spectra of **1** and **2**, respectively. Only diagonal peaks are observed at a mixing time (τ_m) of 20 μs. Cross peaks grow up as the mixing time increases.

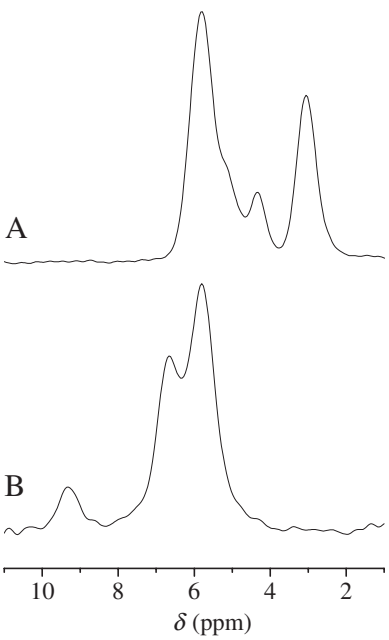

Fig. 1. ^{1}H CRAMPS spectra of (A) **1** and (B) **2**.

In the spectra of **1**, all the cross peaks are observed. Note that the cross peaks of triene (4.4 ppm) and methoxy protons (3.1 ppm) are observed, although their mutual intramolecular distance is large. This suggests that the intermolecular distance between the triene and methoxy groups is relatively short.

The spectra of **2** show strong cross peaks between the 9.3- and 6.7-ppm peaks, while the cross peaks between the 9.3- and 5.8-ppm peaks are negligibly small. The change of the peak shape around 6 ppm demonstrates that the spin diffusion between the 6.7- and 5.8-ppm peaks takes place. These facts suggest that the formyl groups are not near the hexatriene protons of the adjacent molecules.

Analysis of 2D ^{1}H Spin-Exchange NMR Spectra. In this section, we analyze the mixing time dependence of the intensity of the cross peak in 2D ^{1}H spin-exchange NMR spectra quantitatively in order to estimate time constants of spin exchange. Up to now, simulation models and procedures have been proposed to simulate the buildup curves of the cross peak in order to estimate the domain size.[4,10] The domain size is correlated with a square root of the product of the spin-diffusion rate and the time necessary to reach equilibrium. Therefore, reliable values of the spin-diffusion rate are indispensable.[10,15] Similar procedures have been applied to α-glycine to estimate ^{1}H–^{1}H internuclear distances in one molecule.[16] However, both the spin-diffusion rate and the time necessary to reach equilibrium are dependent on the internuclear distances.

In the present case, thus, we have derived formulae by analogy with those in chemical exchange.[17] With increase in the mixing time, the cross peak grows up, consuming the intensity of the diagonal peak in the same f1 position. For a two-component system those intensities are expressed as follows:

$$I_{\mathrm{cross}} = I^0_{\mathrm{cross}}\left\{1 - \exp\left(-\frac{\tau_m}{T_{se}}\right)\right\} \tag{1}$$

$$I_{\mathrm{diag}} = I^0_{\mathrm{diag}}\left\{1 + C\exp\left(-\frac{\tau_m}{T_{se}}\right)\right\} \tag{2}$$

where I_{cross} and I_{diag} are the intensities of the cross peak and the diagonal peak, respectively, the superscript 0 means the intensity at equilibrium, τ_m is the mixing time, and T_{se} is a time constant of spin exchange. The intensity I_{cross} starts from 0 and reaches I^0_{cross}, while I_{diag} starts from $I^0_{\mathrm{diag}}(1 + C)$ and reaches I^0_{diag}. The C value depends on the number of protons, and then it is related with the intensity ratios at equilibrium as follows:

$$C = I^0_{\mathrm{cross}}/I^0_{\mathrm{diag}}. \tag{3}$$

All the protons are assumed to take part in the spin exchange. This assumption is reasonable because no protons are isolated spatially in **1** and **2**. Exactly speaking, the effect of spin-lattice relaxation should be taken into consideration in Eqs. 1 and 2. However, the mixing times used in the present experiments are short enough to neglect the effect of the spin-lattice relaxation. Equations 1–3 are extended to a three-component system, assuming that spin exchanges between cross peaks are neglected, as follows:

$$I_{\mathrm{cross},i} = I^0_{\mathrm{cross}}\left\{1 - \exp\left(-\frac{\tau_m}{T_{se,i}}\right)\right\} \quad (i = 1, 2) \tag{4}$$

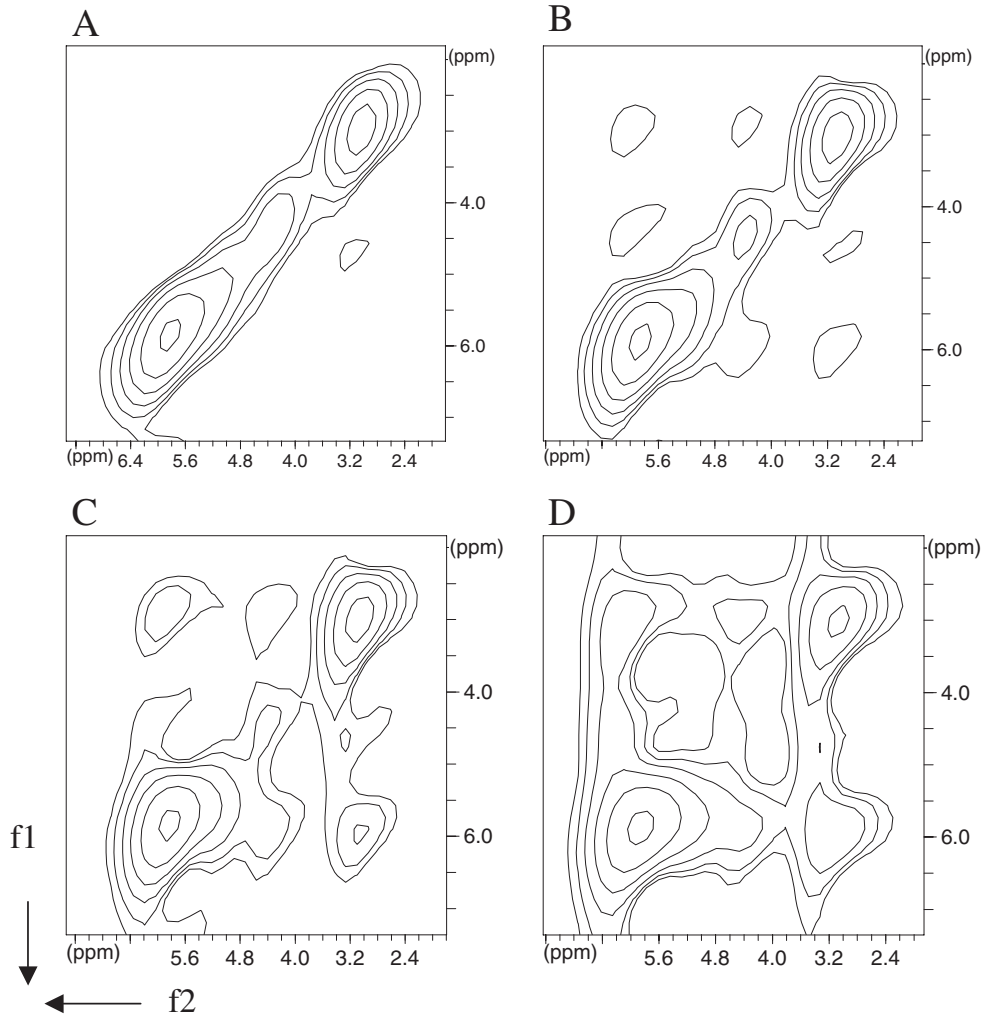

Fig. 2. 2D ^{1}H spin-exchange NMR spectra of **1**. The mixing times were (A) 20, (B) 50, (C) 100, and (D) 200 μs. Six contour plots are drawn from 5% to 90% of the highest peak by multiplying 1.78 for each step.

$$I_{\mathrm{diag}} = I^0_{\mathrm{diag}}\left\{1 + C_1 \exp\left(-\frac{\tau_{\mathrm{m}}}{T_{\mathrm{se},1}}\right) + C_2 \exp\left(-\frac{\tau_{\mathrm{m}}}{T_{\mathrm{se},2}}\right)\right\} \quad (5)$$

$$C_i = I^0_{\mathrm{cross},i}/I^0_{\mathrm{diag}} \quad (i = 1, 2) \quad (6)$$

where the notations are similar to those in Eqs. 1–3.

The ratio of $I_{\mathrm{cross},i}$ to I_{diag} can be obtained with reasonable accuracies in practical experiments. The obtained $I_{\mathrm{cross},i}/I_{\mathrm{diag}}$ ratios are plotted in Figs. 4, 5, and 6 as a function of the mixing time. The cross peak is specified by a notation $\delta_{\mathrm{diag}} \rightarrow \delta_{\mathrm{cross}}$, where δ_{diag} is a chemical shift of the cross peak in the f1 dimension and δ_{cross} is a chemical shift in the f2 dimension. The δ_{diag} value agrees with the chemical shift in the f2 dimension of the diagonal peak. The growth of the cross peak $\delta_{\mathrm{diag}} \rightarrow \delta_{\mathrm{cross}}$ is caused by polarization transfer from a peak at δ_{diag} to that at δ_{cross} in the f2 dimension. In Figs. 4 and 5 the ratios are not plotted for the cross peaks 4.4 → 3.1 ppm for **1** and 6.7 → 5.8 ppm for **2**, because those are masked by neighboring strong peaks.

The plots in Figs. 4, 5, and 6 are analyzed by the following equation;

$$\frac{I_{\mathrm{cross},i}}{I_{\mathrm{diag}}} = \frac{I^0_{\mathrm{cross},i}}{I^0_{\mathrm{diag}}} \cdot \frac{1 - \exp\left(-\frac{\tau_{\mathrm{m}}}{T_{\mathrm{se},i}}\right)}{1 + C_1 \exp\left(-\frac{\tau_{\mathrm{m}}}{T_{\mathrm{se},1}}\right) + C_2 \exp\left(-\frac{\tau_{\mathrm{m}}}{T_{\mathrm{se},2}}\right)}. \quad (i = 1, 2) \quad (7)$$

The values of $I^0_{\mathrm{cross},i}/I^0_{\mathrm{diag}}$ can in principle be estimated from the number of protons. However, those values are corrected for the line width practically, because the peak height is used in this work instead of the integrated intensity. Thus, the $I^0_{\mathrm{cross},i}/I^0_{\mathrm{diag}}$ values are estimated either from a 1D CRAMPS spectrum, from the diagonal peak intensities at a very short mixing time, or from the $I_{\mathrm{cross},i}/I_{\mathrm{diag}}$ value at a very long mixing time. The corrected $I^0_{\mathrm{cross},i}/I^0_{\mathrm{diag}}$ values are listed in Table 1. The C_i value in Eq. 7 can also be estimated from the number of protons, and expresses the fraction of the diagonal peak intensity which moves to the cross peak. The results in Figs. 4 and 5 are fitted by Eq. 7, and the obtained T_{se} values are summarized in Table 1. A single T_{se} value is assumed for each cross peak even when a peak is assigned to two kinds of protons, because of experimental errors. The obtained T_{se} value is considered to

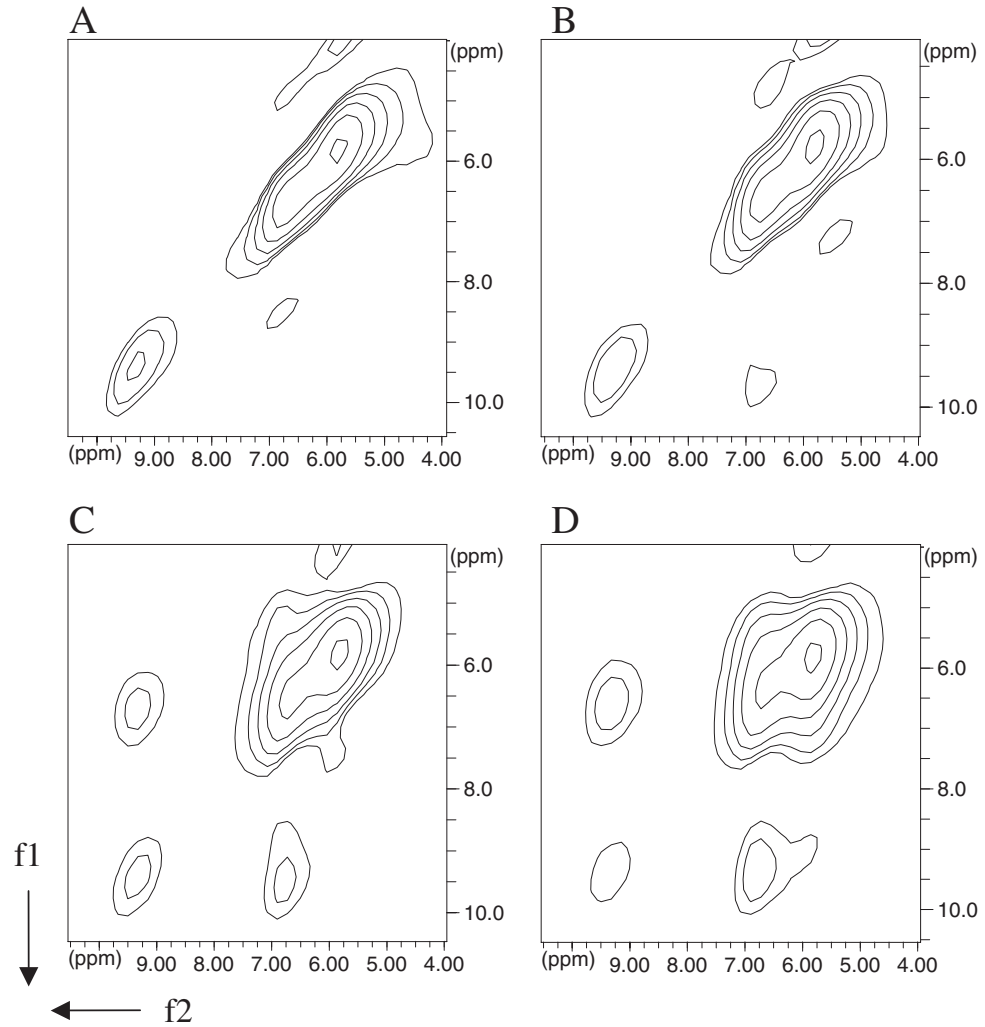

Fig. 3. 2D ^{1}H spin-exchange NMR spectra of **2**. The mixing times were (A) 20, (B) 50, (C) 100, and (D) 200 μs. Six contour plots are drawn from 5% to 90% of the highest peak by multiplying 1.78 for each step.

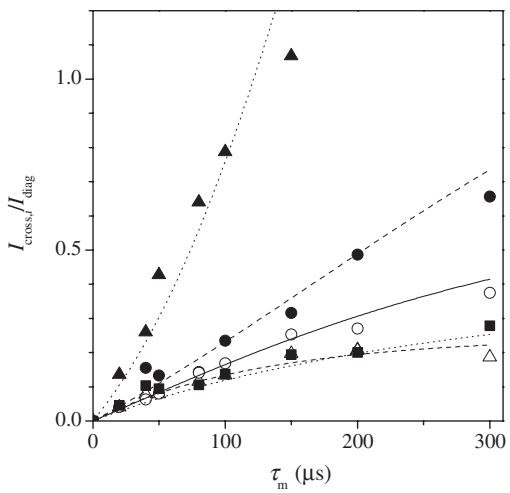

Fig. 4. The mixing time dependence of the $I_{cross,i}/I_{diag}$ ratio for the cross peaks (■) 3.1 → 4.4 ppm, (●) 3.1 → 5.8 ppm, (▲) 4.4 → 5.8 ppm, (○) 5.8 → 3.1 ppm, and (△) 5.8 → 4.4 ppm in **1**. The lines in the figure show fitted results with Eq. 7.

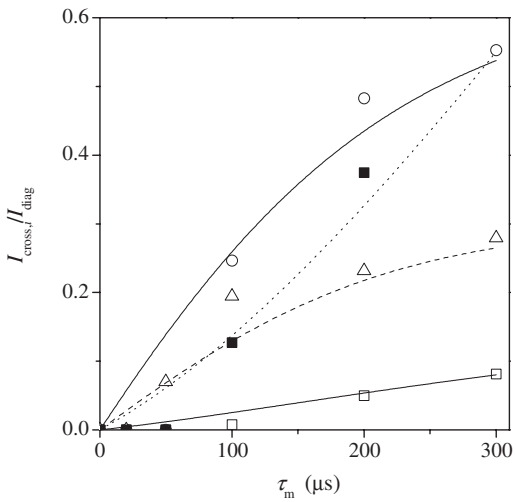

Fig. 5. The mixing time dependence of the $I_{cross,i}/I_{diag}$ ratio for the cross peaks (○) 5.8 → 6.7 ppm, (□) 5.8 → 9.3 ppm, (△) 6.7 → 9.3 ppm, and (■) 9.3 → 5.8 ppm in **2**. The lines in the figure show fitted results with Eq. 7.

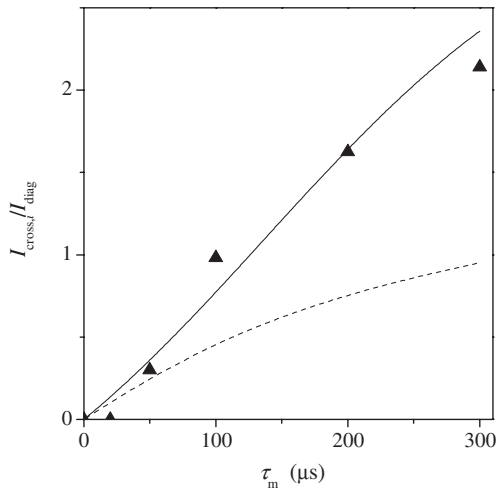

Fig. 6. The mixing time dependence of the $I_{cross,i}/I_{diag}$ ratio for the cross peaks 9.3 → 6.7 ppm in **2**. The chain line and the solid line in the figure show fitted results with Eq. 7 ($T_{se} = 80$ μs) and Eq. 8 ($T_{se} = 125$ μs), respectively.

Table 1. Time Constants for Spin Exchange

Compound	$\delta_{diag} \rightarrow \delta_{cross}$/ppm	R_{eq}[a)]	T_{se}/μs
1 (R = OCH_3)	3.1 → 4.4	0.39	80 ± 30
	3.1 → 5.8	1.5	220 ± 30
	4.4 → 5.8	3.8	80 ± 20[b)]
	5.8 → 3.1	0.67	240 ± 30
	5.8 → 4.4	0.26	80 ± 20
2 (R = CHO)	5.8 → 6.7	0.70	120 ± 20
	5.8 → 9.3	0.21	500 ± 100
	6.7 → 9.3	0.30	80 ± 30[c)]
	9.3 → 5.8	4.7	550 ± 100
	9.3 → 6.7	3.3	125 ± 25[d)]

a) $R_{eq} = I^0_{cross}/I^0_{diag}$. The ratios of the line widths were assumed to be 1.00:0.85:1.33 for the 3.1-, 4.4-, and 5.8-ppm peaks in **1** and 0.85:0.91:1.00 for 5.8-, 6.7-, and 9.3-ppm peaks in **2**. b) The T_{se} value for 4.4 → 3.1 is assumed to be equal to that for 3.1 → 4.4. c) The T_{se} value for 6.7 → 5.8 is assumed to be equal to that for 5.8 → 6.7. d) Eq. 8 is used as described in the text.

reflect the exchange rate for the dominant component. Equation 7 is also applied to the results in Fig. 6, but no good agreement is obtained. The reason is discussed later.

The T_{se} value is inversely proportional to the proton spin exchange rate. The rate of A → B should be equal to that of B → A and, therefore, the T_{se} value of the cross peak A → B should be equal to that of B → A. The obtained T_{se} values in Table 1 satisfy this condition. For **1**, the T_{se} values for 3.1 → 5.8 ppm and 5.8 → 3.1 ppm are 220 and 240 μs, respectively, and those for 4.4 → 5.8 ppm and 5.8 → 4.4 ppm are both 80 μs. Similar agreements are obtained in **2** also. These facts mean that the above treatment is reasonable. Therefore, in the process of analysis, the T_{se} values for 4.4 → 3.1 ppm in **1** and 6.7 → 5.8 ppm in **2** are assumed to be equal to those for 3.1 → 4.4 ppm in **1** and 5.8 → 6.7 ppm in **2**, respectively.

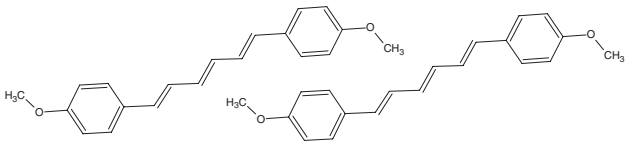

Scheme 2. A model of molecular arrangements in **1**.

The disagreement for the cross peak 9.3 → 6.7 ppm in **2** needs to be discussed. Note that the T_{se} value for 9.3 → 5.8 ppm is much longer than that for 9.3 → 6.7 ppm which is presumed to be about 80 μs from the value for 6.7 → 9.3 ppm. In this case, the two components at 9.3 and 6.7 ppm reach pseudo-equilibrium before the polarization transfer to the 5.8-ppm component starts effectively. Thus, the equations for the two-component system are suitable in this case. The following equation derived from Eqs. 1 and 2 is applied to the growth of the cross peak 9.3 → 6.7 ppm:

$$\frac{I_{cross}}{I_{diag}} = \frac{I^0_{cross}}{I^0_{diag}} \cdot \frac{1 - \exp\left(-\frac{\tau_m}{T_{se}}\right)}{1 + C\exp\left(-\frac{\tau_m}{T_{se}}\right)}. \quad (8)$$

As shown in Fig. 6, Eq. 8 can fit the results well.

Molecular Arrangements. The order of the T_{se} value for **1** is 5.8 ↔ 4.4 ppm (80 μs) ≈ 4.4 ↔ 3.1 ppm (80 μs) < 5.8 ↔ 3.1 ppm (about 230 μs). The peak at 5.8 ppm corresponds mostly to aromatic protons, that at 4.4 ppm to triene protons, and that at 3.1 ppm to methoxy protons. Then, intergroup distances are expected to be in the following increasing order: aromatic protons-triene protons ≈ triene protons-methoxy protons < aromatic protons-methoxy protons. The shortest ^{1}H–^{1}H internuclear distances in a molecule are roughly 0.24 nm for both aromatic protons-triene protons and aromatic protons-methoxy protons. The rotation of the methyl group might make the T_{se} value longer, similarly to the case of α-glycine.[16] It should be noted that the distance between triene protons and methoxy protons is shorter than that between aromatic protons and methoxy protons (about 0.24 nm). Conclusively, a methoxy group is located very close to a hexatriene chain of an adjacent molecule, as illustrated in Scheme 2.

On the other hand, the order of the T_{se} value for **2** is 9.3 ↔ 6.7 ppm (about 100 μs) ≈ 6.7 ↔ 5.8 ppm (120 μs) ≪ 9.3 ↔ 5.8 ppm (about 500 μs). The 9.3-, 6.7-, and 5.8-ppm peaks are assigned to formyl protons, aromatic protons, and mostly triene protons, respectively. Then, intergroup distances are expected to be in the following increasing order: formyl protons-aromatic protons ≈ aromatic protons-triene protons ≪ formyl protons-triene protons. This order reflects the internuclear distances in a molecule, and there are no indications of intermolecular spin exchange between different kinds of groups. The synchrotron X-ray powder diffraction results show that two molecules of **2** form a face-to-face pair and the intermolecular distance between hexatrienes is 0.34–0.36 nm.[1] This structure is consistent with the above NMR results.

Conclusion

2D ^{1}H spin-exchange NMR has been applied to crystalline diphenylhexatrienes. We have estimated the time constants

representing proton spin exchange rates from the analysis of the mixing time dependence of the cross peak intensity. The obtained time constants for **1** demonstrate the presence of an intermolecular spin exchange between triene protons and methoxy protons, and thus reveal that a methoxy group is located close to a hexatriene chain of an adjacent molecule. On the other hand, time constants for **2** reflect the internuclear distances in a molecule, and there are no indications of intermolecular spin exchange between different kinds of groups.

This work demonstrates that 2D ^{1}H spin-exchange NMR is useful to investigate molecular arrangements in organic compounds, especially when the molecule has a rodlike shape.

References

1 Y. Sonoda, Y. Kawanishi, T. Ikeda, M. Goto, S. Hayashi, Y. Yoshida, N. Tanigaki, and K. Yase, *J. Phys. Chem. B*, **107**, 3376 (2003).

2 P. Caravatti, P. Neuenschwander, and R. R. Ernst, *Macromolecules*, **18**, 119 (1985).

3 K. Schmidt-Rohr, J. Clauss, B. Blümich, and H. W. Spiess, *Magn. Reson. Chem.*, **28**, S3 (1990).

4 J. Clauss, K. Schmidt-Rohr, and H. W. Spiess, *Acta Polym.*, **44**, 1 (1993).

5 J. Brus, J. Dybal, P. Schmidt, J. Kratochvil, and J. Baldrian, *Macromolecules*, **33**, 6448 (2000).

6 J. Brus, J. Dybal, P. Sysel, and R. Hobzova, *Macromolecules*, **35**, 1253 (2002).

7 S. M. De Paul, J. W. Zwanziger, R. Ulrich, U. Wiesner, and H. W. Spiess, *J. Am. Chem. Soc.*, **121**, 5727 (1999).

8 D. Huster, X. Yao, and M. Hong, *J. Am. Chem. Soc.*, **124**, 874 (2002).

9 T. Schaller and A. Sebald, *Solid State Nucl. Magn. Reson.*, **5**, 89 (1995).

10 K. Schmidt-Rohr and H. W. Spiess, "Multidimensional Solid-State NMR and Polymers," Academic Press, London (1994).

11 D. P. Burum, D. G. Cory, K. K. Gleason, D. Levy, and A. Bielecki, *J. Magn. Reson., Ser. A*, **104**, 347 (1993).

12 D. J. States, R. A. Haberkorn, and D. J. Ruben, *J. Magn. Reson.*, **48**, 286 (1982).

13 A. G. Redfield and S. D. Kunz, *J. Magn. Reson.*, **19**, 250 (1975).

14 S. Hayashi and K. Hayamizu, *Bull. Chem. Soc. Jpn.*, **64**, 685 (1991).

15 F. Mellinger, M. Wilhelm, and H. W. Spiess, *Macromolecules*, **32**, 4686 (1999).

16 J. Brus, H. Petříčková, and J. Dybal, *Solid State Nucl. Magn. Reson.*, **23**, 183 (2003).

17 R. R. Ernst, G. Bodenhausen, and A. Wokaun, "Principles of Nuclear Magnetic Resonance in One and Two Dimensions," Clarendon, Oxford (1987).